

Contact line motion for partially wetting fluids

Jens Eggers

*School of Mathematics,
University of Bristol, University Walk,
Bristol BS8 1TW, United Kingdom*

We study the flow close to an advancing contact line in the limit of small capillary number. To take into account wetting effects, both long and short-ranged contributions to the disjoining pressure are taken into account. In front of the contact line, there is a microscopic film corresponding to a minimum of the interaction potential. We compute the parameters of the contact line solution relevant to the matching to a macroscopic problem, for example a spreading droplet. The result closely resembles previous results obtained with a slip model.

I. INTRODUCTION

Moving contact lines are encountered in a great number of flow problems, such as spreading of liquid drops [1], dewetting of liquid films [2], coating [3], and sloshing [4]. It was discovered by Huh and Scriven [5] that the viscous dissipation in the fluid wedge bordered by a solid and a fluid-gas interface is logarithmically infinite if the standard hydrodynamic equations and boundary conditions are used [6]. Thus continuum hydrodynamics does not describe the spreading of a drop on a table. Instead, some microscopic length scale must be introduced into the problem.

As a model problem, let us consider the spreading of a viscous drop on a flat substrate. Typical spreading speeds are so small [1] that the bulk of the drop is almost unaffected by viscous shear forces. Hence the drop has the shape of a spherical cap, except in a small region around the contact line [7]. If one extrapolates this spherical cap solution to the contact line, it meets the solid at a well-defined angle, called the “apparent” contact angle θ_{ap} . If for simplicity one assumes that the drop is thin, its radius R is related to θ_{ap} by

$$\theta_{ap} = 4V/(\pi R^3), \quad (1)$$

where V is the volume of the drop.

However, near the contact line the shear rate is of order U/h , where U is the contact line speed and h the local thickness of the fluid film. Near the contact line viscous forces become very large, and strongly bend the interface. A dimensionless measure of this viscous bending is the capillary number $Ca = \eta U/\gamma$, representing a ratio of viscous to capillary forces, with η the viscosity and γ surface tension. As we will show below, within the approximation we adopt here, the slope h' of the interface as function of the distance x from the contact line has the form [8]

$$h'^3(x) = \theta_e^3 + 9Ca \ln(x/L), \quad (2)$$

where θ_e is the equilibrium contact angle and L a microscopic length scale. As illustrated in Fig. 1, we have adopted a coordinate system in which the contact line is at rest. The local description (2) applies for $x/L \gg 1$, i.e. at a distance from the contact line where microscopic details no longer matter.

The distinguishing feature of (2) is that the *curvature* vanishes for $x/L \rightarrow \infty$. This is a necessary condition for the local profile (2) to be matchable to the spherical cap solution that makes up the bulk of the spreading drop [9]. The details of this matching procedure have been given in [10], the result being

$$\theta_{ap}^3 = \theta_e^3 + 9\dot{R}\eta/\gamma \ln[R/(2e^2L)], \quad (3)$$

where $e = 2.718281\dots$. Together with (1), (3) is evidently a differential equation for the radius of the spreading drop. For $\theta_{ap} \gg \theta_e$ equations (1), (3) reproduce Tanner's spreading law [1] $R = At^{1/10}$, neglecting logarithmic corrections in time t . To find an explicit expression for A , it remains to know the length L . In this paper, we are going to compute L for a model that includes both long and short-ranged interactions in the interface potential [2]. This model has recently become popular for the numerical treatment of moving contact line problems [11, 12].

To find L , (2) has to be continued to the contact line, where microscopic effects come into play. Previous calculations [10] have done that for the case of fluid slip over the solid surface [13, 14], which relieves the contact line singularity. In the simplest case of a Navier slip condition [5, 10], described by a slip length λ , the result is $L = 3\lambda/(e\theta_e)$. In [15] we have extended this calculation to higher orders in the capillary number. However, corrections are found to be small in a regime where the underlying lubrication description is still expected to be valid [16]. Apart from the slip length, an angle has to be specified at the contact line,

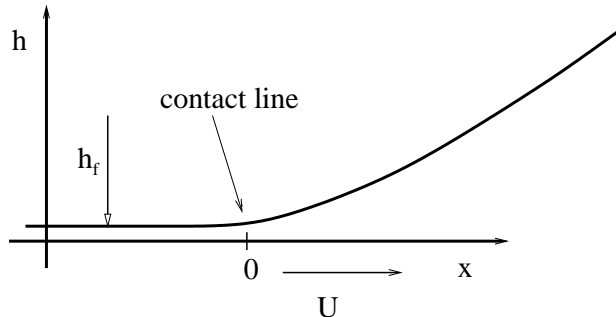


FIG. 1: A cartoon of the contact line. In a frame of reference in which the contact line position is stationary, the solid moves to the right with velocity U . There is a very thin film of thickness h_f in front of the contact line.

which is often taken to be the equilibrium contact angle. This assumption implies that the total dissipation near the contact line is dominated by viscous effects, rather than dissipation localized at the contact line [17].

Here we adopt a model that builds in the equilibrium properties in a more rational way, by including the interface potential into the description. Both the equilibrium contact angle [18] and the equilibrium film thickness h_{eq} are determined by the interface potential. Within the model, even the “dry” substrate is covered by a thin film, corresponding to the minimum of the interface potential. The presence of this film thus formally eliminates the contact line singularity, h_{eq} replacing the slip length λ as the cut-off length. Of course, we do not claim that this is a true resolution of the contact line problem. The thickness h_{eq} is often below the thickness of a single molecule, and even a monomolecular layer is not strictly describable by a continuum theory.

Nevertheless, we believe that it is interesting to investigate the interplay between the interface potential and viscous forces. This has first been done by de Gennes, Hua, and Levinson [19], but only taking into account the long-ranged part of the potential. As a result, the equilibrium contact angle could only be worked in in an ad-hoc fashion, as one needs the full potential to define it. We will see below that our results are in line with the results obtained before [19]. The calculation in [20] is based on a simple energy balance, rather than the systematic expansion performed here. The very recent work [21] treats both the advancing and the receding contact line in a manner very close to ours.

Our paper is organized as follows. After introducing the model description, we recall the

case of a static contact line, relating the equilibrium contact angle to the interface potential. We then outline how the parameter L of (2) may be found in an expansion in the capillary number [15]. Assuming a particular form of the interface potential, we then solve the first order problem explicitly. Finally, we compare to other forms of the interface potential as well as to previous work.

II. LUBRICATION DESCRIPTION

For simplicity, we perform our calculations within the framework of lubrication theory, thus limiting ourselves to the case of small contact angles, as well as small capillary number [22]. Experiment shows that this approximation performs reasonably well up to a capillary number of 0.1 [16]. The lubrication equation reads [11]

$$3\eta\bar{h}_t = - \left[h^3(\gamma\bar{h}_{xx} + \Pi(\bar{h}))_x \right], \quad (4)$$

where $\bar{h}(x, t)$ is the thickness of the fluid film and $\Pi(\bar{h})$ is the disjoining pressure [18]. The origin of (4) is a viscous shear flow, driven by the gradient of the pressure $p = -\gamma\bar{h}_{xx} - \Pi(\bar{h})$. The first term is the usual Laplace pressure, proportional to the curvature of the interface, while the disjoining pressure $\Pi(\bar{h})$ is given by $\Pi(\bar{h}) = \partial V/\partial\bar{h}$, where $V(\bar{h})$ is the effective interface potential of a *flat* film of thickness \bar{h} [2]. Thus as soon as \bar{h} is larger than the range of all the interactions between particles, $\Pi(\bar{h})$ can safely be neglected. However, when \bar{h} is of the order of a few nanometers, the disjoining pressure becomes relevant.

To describe an advancing contact line (cf. Fig. 1), it is convenient to pass into a frame of reference that moves with the contact line speed U :

$$\bar{h}(x, t) = h(x + Ut), \quad (5)$$

giving

$$3Ca h_x = - \left[h^3(h_{xx} + \Pi(h)/\gamma)_x \right]. \quad (6)$$

Integrating once one finds that

$$\frac{3Ca(h - h_f)}{h^3} = - [h_{xx} + \Pi(h)/\gamma]_x, \quad (7)$$

where h_f is the (yet unknown) film thickness ahead of the moving contact line.

III. STATICS

It is instructive to look first at the well-known static case $Ca = 0$. Integrating (7) once more one obtains

$$P_0 = -h_{xx} - \Pi(h)/\gamma, \quad (8)$$

where P_0 is the (constant) pressure in the film (neglecting gravity). We are considering a situation where the film is in contact with a large reservoir (for example a drop) with negligible pressure, hence $P_0 = 0$. Thus in the film we must have $\Pi(h_{eq}) = 0$ (corresponding to a minimum of the interface potential), which defines the equilibrium film thickness h_{eq} .

Now (8) can easily be solved by putting $g(h) = h_x(x)$, giving

$$\frac{\partial g^2}{\partial h} = -2\Pi(h)/\gamma. \quad (9)$$

Integrating (9), we obtain the standard expression [18]

$$\theta_e^2 = -2 \int_{h_{eq}}^{\infty} \Pi(\zeta)/\gamma d\zeta \quad (10)$$

for the equilibrium contact angle, which in the lubrication approximation is to be identified with the slope of the interface: $\theta_e = \tan(h_x(\infty)) \approx h_x(\infty)$. By integrating to infinity, we imply that the macroscopic scale on which θ_e is defined is much larger than h_{eq} .

To be more specific, the disjoining pressure has a long-ranged attractive and a short-ranged repulsive part:

$$\Pi(h) = \frac{A}{6\pi h^3} - \frac{B}{h^\alpha}. \quad (11)$$

The repulsive interaction keeps the film thickness from collapsing to zero. The form of the attractive part is rather universal [7], A being known as the Hamaker constant. The most popular choice for the repulsive part is a power law with $\alpha = 9$, which is motivated by the form of the Lennard-Jones interaction. Recently, enormous progress has been made in determining the constants in (11) for some systems [2]. However, the experiments are not sufficiently accurate to determine the value of the exponent α [23]. For some of the explicit results to be reported below we are going to choose another value, $\alpha = 5$, to be able to perform our calculations analytically. Using the specific form of (11), one easily finds that

$$h_{eq} = (B/A)^{1/(\alpha-3)}, \quad \theta_e^2 = \frac{\alpha - 3}{\alpha - 1} \frac{A}{6\pi\gamma h_{eq}^2}. \quad (12)$$

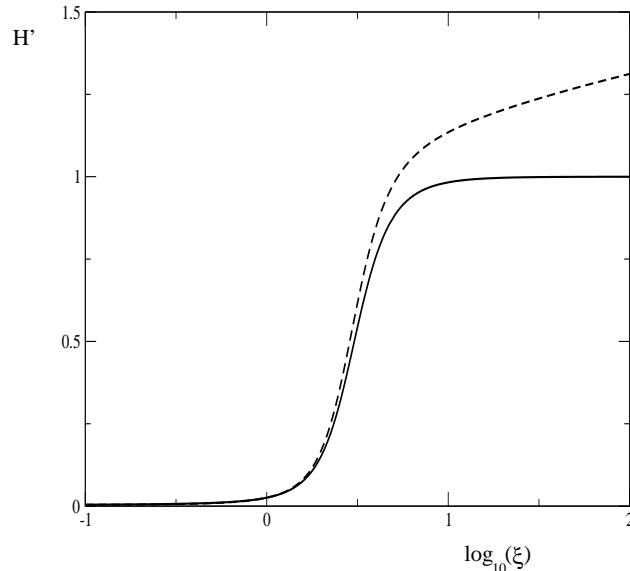


FIG. 2: Numerical solutions for the rescaled interface slope $H(\xi)$. The full line is the static solution (16), the dashed line a solution of (17) for $\delta = 0.1$ and $\alpha = 5$. To expand the horizontal range, a logarithmic scale has been chosen, with $\xi = 0$ shifted somewhat to the left of the contact line position.

To compute the profile, it is useful to introduce new variables, which are scaled to the equilibrium thickness h_{eq} of the film:

$$h(x) = h_{eq}H(\xi), \quad \xi = x\theta_e/h_{eq}. \quad (13)$$

Equation (9) then becomes

$$H'^2 = 2\frac{\alpha - 1}{\alpha - 3} \left(\frac{1}{H^3} - \frac{1}{H^\alpha} \right). \quad (14)$$

To make further progress, we specialize to $\alpha = 5$, in which case we simply have:

$$H' = \frac{H^2 - 1}{H^2}. \quad (15)$$

This can be integrated to give the static interface shape

$$\xi = H + \frac{1}{2} \ln \left(\frac{H - 1}{H + 1} \right), \quad (16)$$

where the left hand side can of course be shifted by an arbitrary amount. The slope of the static interface is shown in Fig.2. To the right of the contact line the slope asymptotes to 1, corresponding to the equilibrium contact angle.

IV. PERTURBATION EXPANSION

Now we turn to the problem of a moving contact line. In the scaled description (13), (7) becomes

$$\frac{\delta(H - H_f)}{H^3} = \left[-H'' + \frac{\alpha - 1}{\alpha - 3} \left(\frac{1}{H^3} - \frac{1}{H^\alpha} \right) \right]', \quad (17)$$

where $\delta = 3Ca/\theta_e^3$ is the rescaled capillary number. In the limit of small h_{eq} the boundaries of the system are pushed out to $\xi = \pm\infty$, and the boundary conditions become

$$H(-\infty) = H_f, \quad H'(-\infty) = 0, \quad H''(\infty) = 0. \quad (18)$$

The first two conditions correspond to the assumption that the liquid forms a film of constant thickness ahead of the contact line. We will see below that it *deviates* slightly from the equilibrium thickness if the contact line is moving. The third boundary condition says that the curvature far away from the contact line is vanishingly small compared to the typical curvature near the contact line, which is $1/h_{eq}$ [15].

We are going to solve (17) in a perturbation expansion in δ , following a procedure adopted before [15]. Of particular interest is the behavior of the solution for large ξ , which corresponds to (2). Namely, for $H \gg 1$ (17) assumes the universal form $\delta/H^2 = H'''$, which has the asymptotic solution [24]

$$H'(\xi) = [3\delta \ln(\xi/\xi_0)]^{1/3}, \quad \xi \gg 1. \quad (19)$$

This solution has vanishing curvature at infinity (as required by (18)), and only contains a single free parameter ξ_0 , to be determined by matching to the contact line. By comparing (19) and (2), one finds

$$\frac{L\theta_e}{h_{eq}} = \xi_0 e^{1/(3\delta)}. \quad (20)$$

On the other hand, the full solution $H(\xi)$ possesses a perturbation expansion in δ around the static profile $H_0(\xi)$:

$$H(\xi) = H_0(\xi) + \delta H_1(\xi) + O(\delta^2). \quad (21)$$

For large ξ , we have $H_0'(\xi) \approx 1$, corresponding to the equilibrium contact angle. By comparing this to (19), we find that $\ln(\xi_0)$ has the following expansion:

$$-3 \ln(\xi_0) = \frac{1}{\delta} + c1 + O(\delta). \quad (22)$$

Substituting into (19), we find that for large ξ

$$H_1'(\xi) = \ln(\xi) + c_1/3. \quad (23)$$

To compute L , we thus take the following steps: First, we solve the full problem (17) perturbatively to obtain $H_1(\xi)$. Then, analyzing H_1 for large ξ , we obtain c_1 , which gives ξ_0 by virtue of (22). Combining this with (20), we finally have

$$L = \frac{h_{eq}}{\theta_e} e^{-c_1/3}. \quad (24)$$

V. EXPLICIT SOLUTION

To first order in δ , (17) becomes

$$\int_{-\infty}^{\xi} \frac{H_0 - 1}{H_0^3} d\xi = -H_1'' + \frac{\alpha - 1}{\alpha - 3} \left(\frac{-3H_1}{H_0^4} + \frac{\alpha H_1}{H_0^{\alpha+1}} \right) + C, \quad (25)$$

where we have integrated once, resulting in a constant of integration C . From now on we consider the special case $\alpha = 5$, for which we can make use of the static solution $H_0(\xi)$ given by (16).

The integral on the left-hand-side of (25) can be performed by exchanging the role of dependent and independent variables using (15):

$$\int_{-\infty}^{\xi} \frac{H_0 - 1}{H_0^3} d\xi = \int_1^{H_0} \frac{dH_0}{H_0(H_0 + 1)} = \ln \left(\frac{2H_0}{H_0 + 1} \right). \quad (26)$$

The limit of (26) for large ξ is $\ln(2)$, hence taking the same limit in (25) yields $C = \ln(2)$ for the constant of integration. Now considering the opposite limit of $\xi \rightarrow -\infty$, and using $H_0(-\infty) = 1$, one finds $H_1(-\infty) = -\ln(2)/4$.

To solve (25), it is useful to rewrite the entire equation using H_0 as the independent variable. To avoid cumbersome expressions, we denote H_0 by the symbol ζ . Thus (25) turns into:

$$F(\zeta) \equiv \ln \left(\frac{\zeta}{\zeta + 1} \right) = -(H_1)_{\zeta\zeta} \left(\frac{\zeta^2 - 1}{\zeta^2} \right)^2 + 2(H_1)_{\zeta} \left(\frac{1}{\zeta^3} - \frac{1}{\zeta^5} \right) + 6H_1 \left(\frac{1}{\zeta^4} - \frac{5}{3\zeta^6} \right). \quad (27)$$

Remarkably, this equation can be solved exactly by noticing that two fundamental solutions are

$$H_1^{(1)} = \frac{16\zeta^5 - 50\zeta^3 + 30\zeta}{\zeta^2(\zeta^2 - 1)} + 15 \frac{\zeta^2 - 1}{\zeta^2} \ln \left(\frac{\zeta - 1}{\zeta + 1} \right) \quad \text{and} \quad H_1^{(2)} = \frac{\zeta^2 - 1}{\zeta^2}, \quad (28)$$

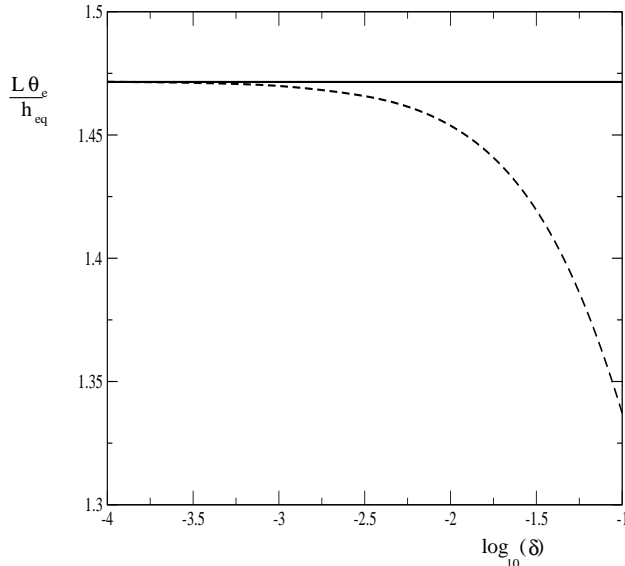


FIG. 3: A comparison with simulation. The full line is the leading-order result of our calculation (34), the dashed line is the numerical result, valid to all orders in δ .

which we found using Maple. Thus a general solution of (27) is

$$H_1 = H_1^{(1)} \left[b_1 - \int_2^\zeta H_1^{(2)} F/W d\zeta' \right] + H_1^{(2)} \left[b_2 + \int_2^\zeta H_1^{(1)} F/W d\zeta' \right], \quad (29)$$

where W is the Wronskian.

The limit $\zeta \rightarrow 1$ corresponds to the thin film. From the condition that H_1 has to remain finite in this limit, one finds

$$b_1 = - \int_1^2 H_1^{(2)} F/W d\zeta' = 3 \ln(3)/16 - \ln(2)/4, \quad (30)$$

since $H_1^{(1)} \rightarrow \infty$ for $\zeta \rightarrow 1$. As shown in the Appendix, the other constant of integration b_2 is determined by the terms of order ζ^0 as $\zeta \rightarrow 1$. In the limit of $\zeta \rightarrow \infty$, on the other hand, one is approaching the bulk fluid, for which we find $H_1^{(1)} \approx 16\zeta$ and $H_1^{(2)} \approx 1$, so a straightforward analysis of (29) yields

$$H_1(\zeta) = \zeta(\ln(\zeta) - 2 \ln(2)) + O(\ln(\zeta)). \quad (31)$$

VI. RESULTS AND DISCUSSION

Now we are in a position to calculate the constant c_1 appearing in (23). From (16) we have $\zeta \equiv H_0 \approx \xi$ for large ξ , and thus

$$H_1'(\zeta) = (\ln(\xi) - 2 \ln(2) + 1) \quad (32)$$

in this limit. We conclude that H_1 indeed has the asymptotic form (23) we anticipated, and we can identify

$$c_1 = 3 - 6 \ln(2). \quad (33)$$

Using (24), we now have

$$L = \frac{4h_{eq}}{e\theta_e}, \quad (34)$$

which is the central result of this paper.

The result (34) can of course be tested by comparing with a numerical solution of the full equation (17). A linear analysis around the film thickness $H = H_f$ reveals an exponentially growing solution

$$H(\xi) = H_f + \epsilon \exp(\gamma\xi), \quad (35)$$

where $\gamma = 2 + O(\delta)$. Any small perturbation of the constant solution $H = H_f, H' = 0, H'' = 0$ will thus lead to an initial growth of the form (35). As $\xi \rightarrow \infty$, the solution generically tends to a finite curvature [24]. Thus H_f has to be adjusted to find the unique solution which obeys the boundary condition (18) at infinity. The asymptotics of this solution of course has to conform with (19).

However, the approach to this solution is very slow, as revealed by the full asymptotic expansion [25]

$$H'(\xi) = [3\delta \ln(\xi/\xi_0)]^{1/3} \left\{ 1 + \sum_{i=2}^{\infty} \frac{b_i}{(\ln(\xi/\xi_0))^i} \right\}. \quad (36)$$

To be consistent with (19), the coefficient b_1 was chosen to vanish, since it would lead to a redefinition of ξ_0 . To obtain ξ_0 numerically, we fitted the numerical solution of (17) to (36), using the first five terms of the expansion. In Fig. 3 we plot the numerical result for L over a wide range of δ -values. For reasonably small δ 's, applicable to most experimental situations, the result is very well approximated by the present first order calculation.

Our analytical approach has of course been limited to the case $\alpha = 5$, which is non-standard. Using the numerical procedure described above, it is a simple matter to obtain L for arbitrary α . Fig.4 shows the result of this calculation in the limit of small δ . As to be expected, the variation with α is not very strong. Large values of α correspond to a very hard core.

Finally, it remains to compare our results to [19], who only took the long-ranged part of the disjoining pressure into account. At the contact line, it was assumed that the solution

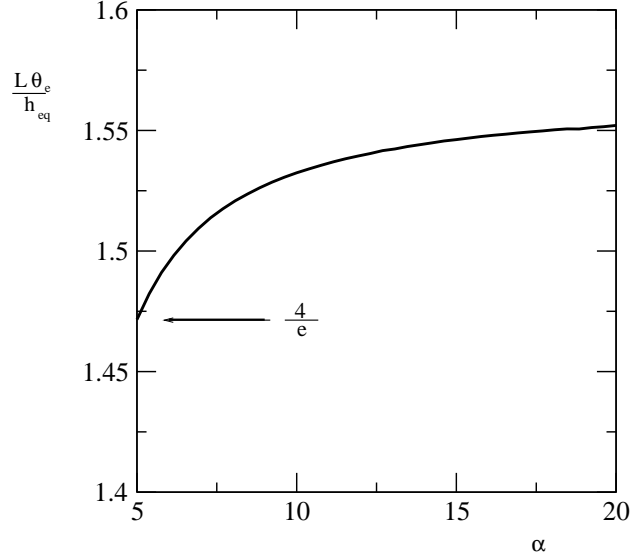


FIG. 4: The characteristic length L as function of the exponent α characterizing the potential. For $\alpha = 5$ the numerical result agrees with (34).

matches to the equilibrium contact angle. The result was reported in the form $L_{GHL} = a/(2\theta_e^2)$, where

$$a = \sqrt{\frac{A}{6\pi\gamma}} \quad (37)$$

is a length scale characterizing the range of van-der-Waals forces. Thus, using (12) the result of [19] can be converted to

$$L_{GHL} = \sqrt{\frac{\alpha - 1}{\alpha - 3}} \frac{h_{eq}}{2\theta_e}, \quad (38)$$

which is essentially the same result as (34), but with a different prefactor. In conclusion, for both a slip and the present thin film model, L is set by the respective microscopic length.

Acknowledgments

I am grateful to Len Pismen for his input, and to the participants of the Thin Film workshop in Udine in 2005, organized by Serafim Kalliadasis and Uwe Thiele, for advice.

APPENDIX

Here we describe how to determine the remaining constant of integration b_2 in (29), by comparing to the asymptotics (35) of the full solution as $\xi \rightarrow -\infty$. Namely, as we have

shown above,

$$H_f = 1 - (\ln(2)/4)\delta + O(\delta^2), \quad (\text{A.1})$$

and it is straightforward to see that the exponent is

$$\gamma = 2 + \gamma_1\delta + O(\delta^2), \quad \gamma_1 = 9 \ln(2)/4 - 1/8. \quad (\text{A.2})$$

Thus at zeroth order in δ one finds $\zeta = 1 + \epsilon \exp(2\xi)$. On the other hand, the full static profile (16) gives $2(\xi - 1 + \ln(2)/2) = \ln(\zeta - 1) + O(\zeta - 1)$. Thus by comparing the two profiles one identifies $\ln(\epsilon) = \ln(2) - 2$.

Expanding (35) to next order in δ leads to

$$\begin{aligned} H_1 = -\ln(2)/4 + \gamma_1(\xi - 1 + \ln(2)/2) \exp[2\xi - 2 + \ln(2)] = \\ -\ln(2)/4 + \gamma_1 \ln(\zeta - 1)(\zeta - 1) + O(\zeta - 1)^2. \end{aligned} \quad (\text{A.3})$$

Thus in the limit of $\zeta \rightarrow 1$, (29) must have the same form as (A.3). The integrals in (29) can be performed using Maple, and in the limit they give

$$H_1 = -\ln(2)/4 + (a + \gamma_1 \ln(\zeta - 1)) (\zeta - 1),$$

which matches (A.3) if $a = 0$. From this requirement we finally get

$$\begin{aligned} b_2 = \frac{107}{192} - \frac{157}{96} \ln(3) - 3 \operatorname{dilog}(2/3) + 3/2 \operatorname{dilog}(4/3) + \\ \frac{15}{16} \operatorname{dilog}(3) + \frac{75}{32} (\ln(3))^2 + \frac{125}{48} \ln(2) - \\ \frac{27}{8} \ln(2) \ln(3) - \frac{15}{16} (\ln(2))^2 + \frac{13}{32} \pi^2 = 0.359777 \dots \end{aligned} \quad (\text{A.4})$$

-
- [1] L. Tanner, *J. Phys. D: Appl. Phys.* **12**, 1473 (1979).
 - [2] R. Seemann, S. Herminghaus, and K. Jacobs, *J. Phys. Condens. Mat.* **13**, 4925 (2001).
 - [3] T. Blake and K. Ruschak, *Nature* **282**, 489 (1979).
 - [4] J. Billingham, *J. Fluid Mech.* **464**, 365 (2002).
 - [5] C. Huh and L. Scriven, *J. Coll. Int. Sci.* **35**, 85 (1971).
 - [6] L. Landau and E. Lifshitz, *Fluid Mechanics* (Pergamon, Oxford, 1984).
 - [7] P. de Gennes, *Rev. Mod. Phys.* **57**, 827 (1985).

- [8] O. Voinov, *Fluid Dynamics* **11**, 714 (1976).
- [9] J. Eggers, *Phys. Fluids* **17**, 082106 (2005).
- [10] L. Hocking, *Q. J. Appl. Math.* **36**, 55 (1983).
- [11] J. Becker, G. Grün, R. Seemann, H. Mantz, K. Jacobs, K. Mecke, and R. Blossey, *Nature Mat.* **2**, 59 (2003).
- [12] U. Thiele and E. Knobloch, *Phys. Fluids* **15**, 892 (2003).
- [13] C. Cottin-Bizonne, B. Cross, A. Steinberger, and E. Charlaix, *Phys. Rev. Lett.* **94**, 056102 (2005).
- [14] J. Koplik, J. Banavar, and J. Willemsen, *Phys. Fluids A* **1**, 781 (1989).
- [15] J. Eggers, *Phys. Fluids* **16**, 3491 (2004).
- [16] Q. Chen, E. Ramé, and S. Garoff, *Phys. Fluids* **7**, 2631 (1995).
- [17] F. Brochard-Wyart and P. de Gennes, *Adv. Colloid Interface Sci.* **9**, 1 (1992).
- [18] J. de Feijter, in *Thin liquid films*, edited by I. Ivanov (Marcel Dekker, New York, 1988).
- [19] P. de Gennes, X. Hua, and P. Levinson, *J. Fluid Mech.* **212**, 55 (1990).
- [20] L. Pismen and Y. Pomeau, *Phys. Fluids* **16**, 2604 (2004).
- [21] L. Pismen and U. Thiele (2005), URL <http://uk.arxiv.org/abs/physics/0509260>.
- [22] A. Oron, S. Davis, and S. Bankoff, *Rev. Mod. Phys.* **69**, 931 (1997).
- [23] R. Seemann, private communication (2005).
- [24] B. Duffy and S. Wilson, *Appl. Math. Lett.* **63**, 63 (1997).
- [25] C. Bender and S. Orszag, *Advanced mathematical methods for scientists and engineers* (Mc Graw-Hill, New York, 1978).